A Novel Detection Criterion for Weak m-Ary Signals and Its Application to UltraWideband Multiple Access Systems

Iickho Song, *Senior Member, IEEE*, Jinkyu Koo, Hyoungmoon Kwon, *Student Member, IEEE*, So Ryoung Park, *Member, IEEE*, Sung Ro Lee, and Bo-Hyun Chung

***Abstract*—In this paper, we propose a novel criterion for the detection of weak m-ary signals. In the sense of minimizing the error probability, the proposed criterion is optimal when the signal strength approaches zero. Based on the proposed criterion, a detection scheme for ultrawideband multiple access systems is proposed and analyzed in the presence of impulsive interference. Numerical results show that the proposed detector requires less complexity than, and possesses almost the same performance as, the maximum likelihood detector. In impulsive interference, the proposed detector also offers significant performance improvement over the detector optimized for a Gaussian environment.**

***Index Terms*—Locally optimum (LO), maximum likehood (ML), ultrawideband (UWB), weak signal detection.**

I. Introduction

WITH SIGNIFICANT interest in developing low-power communication systems, the importance of weak signal detection keeps growing. When the signal is vanishingly small, it is desirable to design a detector with optimum performance at low signal-to-noise ratio (SNR), for which the locally optimum (LO) criterion [1]–[3] can be used. The LO criterion is based on the generalized Neyman–Pearson lemma [2] and, given the false alarm probability, maximizes the detection probability when the signal is of small amplitude. The LO criterion has been extensively studied (e.g., [4]–[7]) because of the advantage of simple detector structures and the almost optimal performance even at large signal strength in many cases. On the other hand, since the LO criterion is derived basically for the detection of binary signals, it is not directly applicable in modern digital communication systems where the receiver should choose among three or more hypotheses.

To overcome such a limit of the binary LO criterion, we propose a novel criterion that is directly useful for the detection of weak m-ary signals, thereby extending the binary LO criterion. The proposed criterion results in simple detector structures in non-Gaussian, impulsive noise environments, and is optimum when the signals are of weak strengths. Here, unlike in the binary LO criterion, the term "optimum" is in the sense of minimum error probability.

We also address an application of the proposed criterion in ultrawideband multiple access (UWB-MA) systems. The UWB-MA systems operating in an extremely broad frequency range from near dc to a few gigahertz should not interfere with narrow-band communication systems operating in dedicated bands while contending with a variety of interfering signals. These requirements necessitate the use of spread-spectrum techniques and consequently result in signals of extraordinarily small strength with a natural request for low power consumption. Therefore, design of weak signal detectors for UWB-MA systems is much more important than that for other communication systems.

In the UWB-MA systems, the sum of the multiple access interference (MAI) and channel noise is modeled as impulsive interference [8] based on the impulse-like feature of UWB pulses [9], [10] and actual measurements of the ambient channel noise [11]. The impulsive modeling has proved appropriate when the number of users in the communication links is small, and the central limit theorem cannot be applied. Clearly, due to the impulsive environment in the UWB-MA systems, the conventional detector optimized for the Gaussian environment [the Gaussian-optimized (GO) detector] could experience severe performance degradation in the UWB-MA systems.

Based on the novel criterion, we propose a new detector for UWB-MA systems in the presence of impulsive interference. We shall observe that the performance of the proposed detector barely differs from that of the optimal detector despite the fact that proposed detector is a low-complexity version of the optimal detector. Computer simulations also show that the proposed detector generally outperforms the Gaussian-optimized detector in impulsive interference.

Manuscript received July 2, 2004; revised December 19, 2004, and January 30, 2005. This work was supported by Korea Science and Engineering Foundation (KOSEF) under Grant R01-2004-000-10019-0. The review of this paper was coordinated by Dr. C. Tepedelenlioglu.

I. Song, J. Koo, and H. Kwon are with the Department of Electrical Engineering, Korea Advanced Institute of Science and Technology (KAIST), Daejeon, Korea (e-mail: i.song@ieee.org; jkoo@Sejong.kaist.ac.kr; kwon@Sejong.kaist.ac.kr).

S. R. Park is with the School of Information, Communications, and Electronics Engineering, the Catholic University of Korea (CUK), Bucheon, Korea.

S. R. Lee is with the Division of Information, Mokpo National University, Muan, Korea.

B.-H. Chung is with the Mathematics Section, College of Science and Technology, Hongik University, Jochiweon, Korea.

Digital Object Identifier 10.1109/TVT.2005.858165

II. Novel Criterion for Weak m-Ary Signals

A. Observation Model

Fig. 1 describes a demodulator decomposing the received signal into an N-dimensional vector and a detector making a decision on the transmitted signal in each symbol interval T_s. Specifically, the received signal is correlated by a series of N

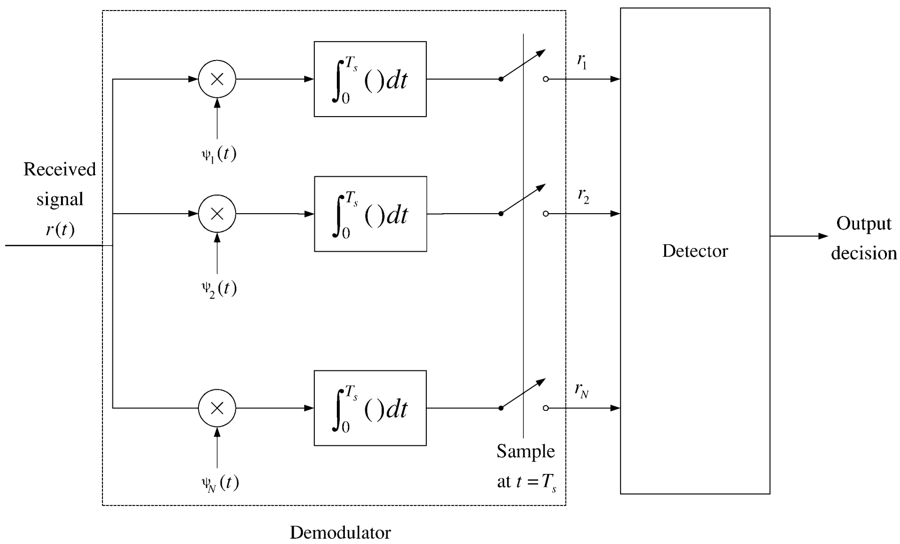

Fig. 1. Demodulator and detector.

orthonormal basis functions $\{\psi_k(t)\}_{k=1}^N$ in the demodulator, the outputs of which are then used for the detector to make a decision. It is assumed that the N basis functions span the signal space. In other words, for any signal in the set $\{s_i(t)\}_{i=1}^M$ of $M \geq 2$ possible signals, there exists a unique set $\{c_{ik}\}_{k=1}^N$ of real numbers such that $s_i(t) = \sum_{k=1}^N c_{ik}\psi_k(t)$. The dimensionality N of the signal space will be equal to M if all the signals $\{s_i(t)\}_{i=1}^M$ are linearly independent; otherwise, we have $N < M$.

Suppose a signal $s_i(t)$ has passed through an additive channel to produce the received signal

$$r(t) = \theta_i \tilde{s}_i(t) + n(t), \quad 0 \leq t \leq T_s \tag{1}$$

where $n(t)$ is the sample function of the additive noise, $\theta_i = \sqrt{\int_0^{T_s} |s_i(t)|^2\, dt}$ is the strength of $s_i(t)$, and $\tilde{s}_i(t)$ represents the unit energy version of $s_i(t)$. Assume that the signal strength θ_i can be expressed as

$$\theta_i = \theta\epsilon_i, \quad i = 1, 2, \ldots, M \tag{2}$$

where θ is the common factor of $\{\theta_i\}_{i=1}^M$, and $\{\epsilon_i\}_{i=1}^M$ are non-negative proportionality constants. In essence, the signal strengths $\{\theta_i\}_{i=1}^M$ can be controlled by θ.

The demodulator in Fig. 1 computes the projections $\{r_k\}_{k=1}^N$ of $r(t)$ onto the N basis functions $\{\psi_k(t)\}_{k=1}^N$ as

$$r_k = \theta\epsilon_i s_{ik} + n_k, \quad k = 1, 2, \ldots, N \tag{3}$$

where

$$s_{ik} = \int_0^{T_s} \tilde{s}_i(t)\psi_k(t)\, dt, \quad k = 1, 2, \ldots, N \tag{4}$$

are the signal components, and $n_k = \int_0^{T_s} n(t)\psi_k(t)\, dt, k = 1, 2, \ldots, N$ are the noise components. The demodulator output vector $\mathbf{r} = (r_1, r_2, \ldots, r_N)$ can be expressed as

$$\mathbf{r} = \theta\epsilon_i \mathbf{s}_i + \mathbf{n} \tag{5}$$

where $\mathbf{s}_i = (s_{i1}, s_{i2}, \ldots, s_{iN})$ is the vector of signal components, and $\mathbf{n} = (n_1, n_2, \ldots, n_N)$ is the vector of noise components. Note that we have

$$\begin{aligned} \sum_{k=1}^N s_{ik}^2 &= \sum_{k=1}^N s_{ik}^2 \int_0^{T_s} |\psi_k(t)|^2\, dt \\ &= \int_0^{T_s} \left(\sum_{k=1}^N s_{ik}\psi_k(t)\right)\left(\sum_{k=1}^N s_{ik}\psi_k(t)\right) dt \\ &= \int_0^{T_s} |\tilde{s}_i(t)|^2\, dt \\ &= 1. \end{aligned} \tag{6}$$

Four typical signaling schemes and the corresponding parameters are shown in Appendix A.

B. Proposed Criterion

Suppose that the m-ary signals $\{s_i(t)\}_{i=1}^M$ are equi-probable, that is, the *a priori* probability of a signal being transmitted is $1/M$. The probability $P_e(\theta)$ of symbol error is then given as

$$P_e(\theta) = 1 - \frac{1}{M}\sum_{i=1}^M \int_{D_i} p(\mathbf{r} \mid s_i, \theta)\, d\mathbf{r} \tag{7}$$

where D_i is the N-dimensional decision region over which we decide $s_i(t)$ is sent, and $p(\mathbf{r} \mid s_i, \theta)$ represents the conditional probability density function (pdf) of $\mathbf{r}$ given that $s_i(t)$ is transmitted when the signal strength parameter is θ. Here, $\{D_i\}_{i=1}^M$ is a partition of the N-dimensional space $\mathbb{R}^N$. If $\theta = 0, p(\mathbf{r} \mid s_i, 0)$ is equal to $p_{\mathbf{n}}(\mathbf{r})$ from (5), where $p_{\mathbf{n}}(\cdot)$ denotes the pdf of $\mathbf{n}$. Thus, we have

$$\begin{aligned} P_e(0) &= 1 - \frac{1}{M}\sum_{i=1}^M \int_{D_i} p(\mathbf{r} \mid s_i, 0)\, d\mathbf{r} \\ &= 1 - \frac{1}{M}\int_{\mathbb{R}^N} p_{\mathbf{n}}(\mathbf{r})\, d\mathbf{r} \\ &= 1 - \frac{1}{M} \end{aligned} \tag{8}$$

a constant independent of the criterion. Based on this observation, we have the following.

Proposition 1: When the signal strength approaches zero, $P_e(\theta)$ is minimized if, for $i = 1, 2, \ldots, M$

$$D_i = \left\{ \mathbf{r} : \left. \frac{\partial}{\partial \theta} p(\mathbf{r} \mid s_i, \theta) \right|_{\theta=0} \geq \left. \frac{\partial}{\partial \theta} p(\mathbf{r} \mid s_j, \theta) \right|_{\theta=0}, \quad \forall j \right\}. \tag{9}$$

Proof: Since

$$P_e(\theta) \approx P_e(0) + \theta \left. \frac{\partial}{\partial \theta} P_e(\theta) \right|_{\theta=0} \tag{10}$$

a criterion minimizing $(\partial)/(\partial\theta) P_e(\theta)|_{\theta=0}$ would result in the minimum $P_e(\theta)$ when θ is close to zero. Now, since

$$\begin{aligned} &\left. \frac{\partial}{\partial \theta} P_e(\theta) \right|_{\theta=0} \\ &= -\frac{1}{M} \sum_{i=1}^{M} \left. \left(\frac{\partial}{\partial \theta} \int_{D_i} p(\mathbf{r} \mid s_i, \theta)\, d\mathbf{r} \right) \right|_{\theta=0} \\ &= -\frac{1}{M} \sum_{i=1}^{M} \int_{D_i} \left(\left. \frac{\partial}{\partial \theta} p(\mathbf{r} \mid s_i, \theta) \right|_{\theta=0} \right) d\mathbf{r} \end{aligned} \tag{11}$$

$(\partial)/(\partial\theta) P_e(\theta)|_{\theta=0}$ is minimized if D_i is as specified in (9). Q.E.D

The decision region (9) tells us that $P_e(\theta)$ is minimized by selecting $s_i(t)$ if $(\partial)/(\partial\theta) p(\mathbf{r} \mid s_i, \theta)|_{\theta=0}$ is larger than or equal to $(\partial)/(\partial\theta) p(\mathbf{r} \mid s_j, \theta)|_{\theta=0}$ for all j when $\theta \to 0$.

Proposition 2: Let D_i^P and D_i^{ML} be the decision regions of the proposed and maximum-likelihood (ML) criteria, respectively. Then

$$D_i^P = \lim_{\theta \to 0} D_i^{\mathrm{ML}}. \tag{12}$$

Proof: Since $p(\mathbf{r} \mid s_i, \theta) = \sum_{m=0}^{\infty} (\theta^m)(m!) \cdot (\partial^m)/(\partial\theta^m)$ $p(\mathbf{r} \mid s_i, \theta)|_{\theta=0}$, we have

$$\begin{aligned} D_i^{\mathrm{ML}} &= \{ \mathbf{r} : p(\mathbf{r} \mid s_i, \theta) \geq p(\mathbf{r} \mid s_j, \theta), \quad \forall j \} \\ &= \left\{ \mathbf{r} : \left. \frac{\partial}{\partial \theta} p(\mathbf{r} \mid s_i, \theta) \right|_{\theta=0} \right. \\ &\qquad + \frac{\theta}{2} \cdot \left. \frac{\partial^2}{\partial \theta^2} p(\mathbf{r} \mid s_i, \theta) \right|_{\theta=0} + \cdots \\ &\quad \geq \left. \frac{\partial}{\partial \theta} p(\mathbf{r} \mid s_j, \theta) \right|_{\theta=0} \\ &\qquad \left. + \frac{\theta}{2} \cdot \left. \frac{\partial^2}{\partial \theta^2} p(\mathbf{r} \mid s_j, \theta) \right|_{\theta=0} + \cdots, \quad \forall j \right\} \end{aligned} \tag{13}$$

from which we easily obtain (12). Q.E.D

An interesting property of the proposed criterion defined by (9) is presented in the following proposition.

Proposition 3: If the joint pdf $p_{\mathbf{n}}(x_1, x_2, \ldots, x_N)$ of the noise vector $\mathbf{n}$ is a unimodal function of $\|\mathbf{x}\|^2 = \sum_{k=1}^{N} x_k^2$ with the maximum at $\|\mathbf{x}\| = 0$, then the proposed and ML criteria result in the same decision region when the M-ary signals all have the same energy (i.e., when $\epsilon_i = \epsilon$).

Proof: We are to prove that $D_i^{\mathrm{ML}} = D_i^P$. Now, $p_{\mathbf{n}}(x_1, x_2, \ldots, x_N)$ can be rewritten as $p_{\mathbf{n}}(x_1, x_2, \ldots, x_N) = f_u(\|\mathbf{x}\|^2)$, where $f_u(x)$ is a unimodal function of x with the peak at $x = 0$. Without loss of generality, we can assume that $(d)/(dx) f_u(x) \neq 0$ for all $x \neq 0$ and f_u is symmetric. Then, using $p(\mathbf{r} \mid s_i, \theta) = p_{\mathbf{n}}(\mathbf{r} - \theta\epsilon\mathbf{s}_i)$, we have

$$\begin{aligned} D_i^{\mathrm{ML}} &= \left\{ \mathbf{r} : f_u\left(\|\mathbf{r} - \theta\epsilon\mathbf{s}_i\|^2 \right) \geq f_u\left(\|\mathbf{r} - \theta\epsilon\mathbf{s}_j\|^2 \right), \quad \forall j \right\} \\ &= \left\{ \mathbf{r} : \|\mathbf{r} - \theta\epsilon\mathbf{s}_i\|^2 \leq \|\mathbf{r} - \theta\epsilon\mathbf{s}_j\|^2, \quad \forall j \right\} \\ &= \left\{ \mathbf{r} : \sum_{k=1}^{N} (s_{ik} - s_{jk}) r_k \geq 0, \quad \forall j \right\}. \end{aligned} \tag{14}$$

Now, the derivative of $p(\mathbf{r} \mid s_i, \theta)$ with respect to θ is

$$\begin{aligned} &\left. \frac{\partial}{\partial \theta} p(\mathbf{r} \mid s_i, \theta) \right|_{\theta=0} \\ &\quad = \left. \frac{d}{d\left(\|\mathbf{r} - \theta\epsilon\mathbf{s}_i\|^2 \right)} f_u\left(\|\mathbf{r} - \theta\epsilon\mathbf{s}_i\|^2 \right) \right|_{\theta=0} \\ &\qquad \cdot \sum_{k=1}^{N} (-2\epsilon r_k s_{ik}) \end{aligned} \tag{15}$$

at $\theta = 0$. Since

$$\left. \frac{d\, f_u\left(\|\mathbf{r} - \theta\epsilon\mathbf{s}_i\|^2 \right)}{d\left(\|\mathbf{r} - \theta\epsilon\mathbf{s}_i\|^2 \right)} \right|_{\theta=0} = \left. \frac{d\, f_u\left(\|\mathbf{x}\|^2 \right)}{d\left(\|\mathbf{x}\|^2 \right)} \right|_{\|\mathbf{x}\|^2 = \|\mathbf{r}\|^2} \tag{16}$$

we get

$$\begin{aligned} D_i^P &= \left\{ \mathbf{r} : \left. \frac{\partial}{\partial \theta} p(\mathbf{r} \mid s_i, \theta) \right|_{\theta=0} \geq \left. \frac{\partial}{\partial \theta} p(\mathbf{r} \mid s_j, \theta) \right|_{\theta=0}, \quad \forall j \right\} \\ &= \left\{ \mathbf{r} : \left\{ \left. \frac{d}{d\left(\|\mathbf{x}\|^2 \right)} f_u\left(\|\mathbf{x}\|^2 \right) \right|_{\|\mathbf{x}\|^2 = \|\mathbf{r}\|^2} \right\} \right. \\ &\qquad \cdot \sum_{k=1}^{N} (-2\epsilon r_k s_{ik}) \\ &\quad \geq \left\{ \left. \frac{d}{d\left(\|\mathbf{x}\|^2 \right)} f_u\left(\|\mathbf{x}\|^2 \right) \right|_{\|\mathbf{x}\|^2 = \|\mathbf{r}\|^2} \right\} \\ &\qquad \left. \cdot \sum_{k=1}^{N} (-2\epsilon r_k s_{jk}), \quad \forall j \right\} \\ &= \left\{ \mathbf{r} : \sum_{k=1}^{N} (s_{ik} - s_{jk}) r_k \geq 0, \quad \forall j \right\} \end{aligned} \tag{17}$$

which is the same as D_i^{ML}. Q.E.D.

Proposition 3 essentially tells us a sufficient condition under which the performance of the proposed and ML criteria is the same, irrespective of the signal strength.

Corollary 1: In the additive white Gaussian noise (AWGN), the proposed and ML criteria cause exactly the same decision region when the m-ary signals have the same energy.

Proof: The components of $\mathbf{n}$ are independent and identically distributed (i.i.d.) Gaussian variables. Clearly, the joint pdf of $\mathbf{n}$ is a special case of $p_{\mathbf{n}}(\cdot)$ prescribed in Proposition 3. Q.E.D

For the phase shift keyed (PSK) signals, the observation vector $\mathbf{r}$ can be expressed as $\mathbf{r} = (\theta\cos(2\pi i/M) + n_1, \theta\sin(2\pi i/M) + n_2)$ when $s_i(t)$ is sent. Let the joint pdf of n_1 and n_2 be the bivariate Cauchy pdf

$$f(x,y) = \frac{\gamma}{2\pi}\cdot\frac{1}{(x^2+y^2+\gamma^2)^{3/2}} \tag{18}$$

which satisfies the condition specified in Proposition 3. We can easily obtain

$$\begin{aligned} D_i^{\mathrm{ML}} &= D_i^P \\ &= \{\mathbf{r} : r_1\cos(2\pi i/M) + r_2\sin(2\pi i/M) \\ &\quad \geq r_1\cos(2\pi j/M) + r_2\sin(2\pi j/M), \quad \forall j\} \end{aligned} \tag{19}$$

confirming Proposition 3.

The multivariate t-pdf [12]

$$p_{\mathbf{n}}(x_1,x_2,\ldots,x_N) = \frac{\Gamma((\nu+N)/2)}{(\pi\nu)^{N/2}\Gamma(\nu/2)} \cdot \left(1+\nu^{-1}\sum_{k=1}^{N}x_k^2\right)^{-(\nu+N)/2} \tag{20}$$

where $\nu > 0$ denotes the degree of freedom, also satisfies the condition in Proposition 2. Consequently, the proposed and ML criteria will have the same decision region with a set of equienergy signals. Note that (20) becomes a multivariate Cauchy pdf when $\nu = 1$. Still another class of pdfs satisfying the conditions in Proposition 3 is the class of the symmetric α-stable (SαS) pdf [8], which will be considered in some detail in Section III.

C. Examples of the Decision Regions

We now obtain specific examples of the proposed decision regions when the noise components $\{n_k\}_{k=1}^N$ are i.i.d. with the Gaussian, Cauchy, t-, and logistic distributions. Here, the Cauchy, t-, and logistic pdf belong to the class of heavy-tailed pdfs (tails decaying at lower rate than those of the Gaussian pdf) and have been used frequently in the modeling of impulsive environments. In addition, the t-distribution arises naturally in sampling from a Gaussian distributed population [3]. In each case, the decision region of the proposed criterion is compared with that of the ML criterion to help us gain insight into the proposed criterion.

1) Detection in Gaussian Noise: For the common pdf

$$f(x) = \frac{1}{\sqrt{2\pi\sigma^2}}e^{-\frac{x^2}{2\sigma^2}} \tag{21}$$

we have $p(\mathbf{r}\,|\,s_i,\theta) = \exp\{-(1)/(2\sigma^2)\sum_{k=1}^{N}(r_k - \theta\epsilon_i s_{ik})\}$. Thus, we can obtain

$$D_i^{\mathrm{ML}} = \left\{\mathbf{r} : \sum_{k=1}^{N}(\epsilon_i s_{ik} - \epsilon_j s_{jk})r_k \geq \frac{\left(\epsilon_i^2 - \epsilon_j^2\right)\theta}{2}, \quad \forall j\right\} \tag{22}$$

using (6) and

$$D_i^P = \left\{\mathbf{r} : \sum_{k=1}^{N}(\epsilon_i s_{ik} - \epsilon_j s_{jk})r_k \geq 0, \quad \forall j\right\}. \tag{23}$$

2) Detection in Cauchy Noise: For the common Cauchy pdf with zero median

$$f(x) = \frac{\gamma}{\pi(x^2+\gamma^2)} \tag{24}$$

where $\gamma > 0$ is the dispersion parameter determining the spread of the distribution [8], [13]. In this case, it is straightforward to have

$$D_i^{\mathrm{ML}} = \left\{\mathbf{r} : \prod_{k=1}^{N}\frac{(r_k - \theta\epsilon_j s_{jk})^2 + \gamma^2}{(r_k - \theta\epsilon_i s_{ik})^2 + \gamma^2} \geq 1, \quad \forall j\right\} \tag{25}$$

and

$$D_i^P = \left\{\mathbf{r} : \sum_{k=1}^{N}\frac{(\epsilon_i s_{ik} - \epsilon_j s_{jk})r_k}{r_k^2 + \gamma^2} \geq 0, \quad \forall j\right\}. \tag{26}$$

3) Detection in t-Distributed Noise: Let us now assume the common pdf

$$f(x) = \frac{\Gamma((\nu+1)/2)}{\sqrt{\pi\nu}\,\Gamma(\nu/2)}(1+x^2/\nu)^{-(\nu+1)/2}. \tag{27}$$

After some steps, we obtain the decision regions

$$D_i^{\mathrm{ML}} = \left\{\mathbf{r} : \prod_{k=1}^{N}\frac{1+(r_k - \theta\epsilon_j s_{jk})^2/\nu}{1+(r_k - \theta\epsilon_i s_{ik})^2/\nu} \geq 1, \quad \forall j\right\} \tag{28}$$

and

$$D_i^P = \left\{\mathbf{r} : \sum_{k=1}^{N}\frac{(\epsilon_i s_{ik} - \epsilon_j s_{jk})r_k}{1 + r_k^2/\nu} \geq 0, \quad \forall j\right\}. \tag{29}$$

Note that (29) is essentially the same as (26): this is because the Cauchy noise is a special case of the t-noise.

4) Detection in Logistic Noise: We can obtain

$$D_i^{\mathrm{ML}} = \left\{\mathbf{r} : \prod_{k=1}^{N} e^{b\theta(\epsilon_i s_{ik} - \epsilon_j s_{jk})} \cdot \frac{\left(1+e^{-b(r_k - \theta\epsilon_j s_{jk})}\right)^2}{\left(1+e^{-b(r_k - \theta\epsilon_i s_{ik})}\right)^2} \geq 1, \quad \forall j\right\} \tag{30}$$

and

$$D_i^P = \left\{\mathbf{r} : \sum_{k=1}^{N}(\epsilon_i s_{ik} - \epsilon_j s_{jk})\frac{1-e^{-br_k}}{1+e^{-br_k}} \geq 0, \quad \forall j\right\} \tag{31}$$

for the logistic pdf with zero mean

$$f(x) = \frac{be^{-bx}}{(1+e^{-bx})^2} \tag{32}$$

where $b > 0$ and the variance of the distribution is $\pi^2/(3b^2)$.

D. Discussion

In general, D_i^{ML} is dependent on θ as we have observed in (22) and (25) for example, while D_i^P does not depend on θ as we have observed in (23) and (26). This implies that if we use the ML criterion, the value of θ has to be estimated and the performance of a detector with an inaccurate estimate of θ could deviate far from the optimum. Without having to estimate the value of θ and possessing simpler test statistics, the detector using the proposed criterion requires less computational complexity in comparison with the ML detector. In addition, we shall see in Section III that the performance difference between the detectors using the proposed and ML criteria is negligible.

Appendix B illustrates decision regions of the proposed and ML criteria more specifically when the signaling schemes are specified. It is observed that the proposed and ML criteria result in the same decision regions for the PSK and orthogonal signals in the Gaussian environment as expected from Corollary 1. We can also observe that, depending on the interference model and signaling scheme, the proposed and ML criteria might result in the same decision regions, even when the conditions of Proposition 3 are not satisfied: The case of orthogonal signals in logistic interference is one such example.

III. Application to UWB-MA Systems

A. System Model

Assume that the users employ binary pulse position modulation (PPM) in which the transmitted signals consist of a low duty-cycle sequence of a large number of UWB pulses. The duration T_q of the unit energy UWB pulse $q(t)$ is only a very small portion of the frame time (or pulse repetition period) T_f. Since we focus on the detection structure after the demodulation process, we are not concerned with the shape of the UWB pulses.

The lth user's signal for $0 \le t \le N_s T_f$ is one of the two equiprobable signals

$$s_i^{(l)}(t) = \tilde{\theta} \sum_{k=0}^{N_s-1} q\left(t - kT_f - c_k^{(l)} T_c - d_i^{(l)} T_c/2\right) \qquad (33)$$

$i = 1, 2$. Here, N_s is the number of the UWB pulses modulated by a given symbol, $T_s = N_s T_f$ is the symbol duration, $\tilde{\theta}$ is the signal strength when a signal is transmitted, T_c is the chip duration ($T_c > 2T_q$), $\{c_k^{(l)}\}_{k=0}^{N_s-1}$ is the time-hopping sequence of the lth user having period N_c (i.e., $0 \le c_k^{(l)} \le N_h$ and $c_{k+jN_c}^{(l)} = c_k^{(l)}$, for all integers k, j with N_h an integer), $d_1^{(l)} = 0$, and $d_2^{(l)} = 1$. The frame time T_f is chosen to be sufficiently large ($T_f > N_h T_c + T_c$) to reduce intersymbol and intrasymbol interference caused by the delay spread. The difference $T_f - (N_h + 1)T_c$ is called the guard interval. Note that N_c is the theoretical maximum number of users who can be simultaneously active in the system. The descriptions given here are illustrated in Figs. 2 and 3.

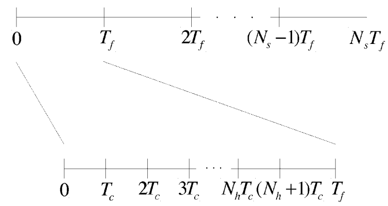

Fig. 2. Profile of a symbol duration, where $T_s = N_s T_f$ is the symbol duration, T_c is the chip duration, and $T_f - (N_h + 1)T_c$ is the guard interval.

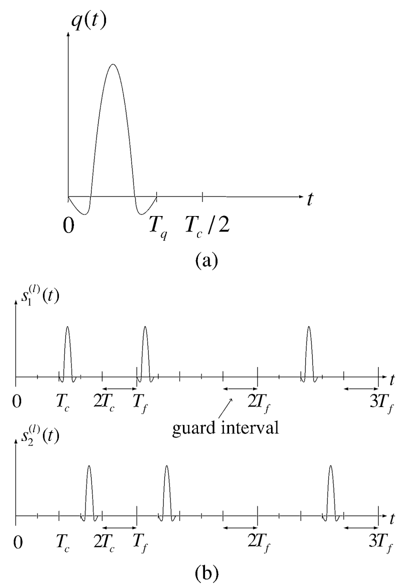

Fig. 3. Example of the signal waveform. (a) Unit energy UWB pulse $q(t)$. (b) lth user's signals $s_1^{(l)}(t)$ and $s_2^{(l)}(t)$ for a symbol duration $T_s = N_s T_f = 3T_f$ when $N_c = 2$, $N_h = 1$, $N_s = 3$, and $(c_0^{(l)}, c_1^{(l)}) = (1, 0)$.

When the UWB-MA system has N_u users ($N_u \le N_c$), the received signal $r(t)$ is given as

$$r(t) = \sum_{l=1}^{N_u} s_{\mathrm{rec}}^{(l)}(t) + \tilde{n}(t), \qquad (34)$$

where $s_{\mathrm{rec}}^{(l)}(t)$ is the lth user's signal at the receiver, and $\tilde{n}(t)$ denotes the channel noise. Let us assume that there is no signal distortion due to the propagation through the channel and that the receiver is interested in determining the data $\{d_i^{(1)}\}$ sent by the first user. Then, the received signal $r(t)$ given that $s_i^{(1)}(t)$ is transmitted can be expressed as

$$r(t) = A_1 s_i^{(1)}(t - \tau_1) + n(t). \qquad (35)$$

In (35), τ_1 represents the time delay between the transmitter of the first user and the receiver, A_1 models the attenuation of the first user's signal over the channel, and

$$n(t) = \sum_{l=2}^{N_u} s_{\mathrm{rec}}^{(l)}(t) + \tilde{n}(t) \qquad (36)$$

is the total interference against determining $\{d_i^{(1)}\}$. On the right-hand side of (36), the first term is the MAI due to other users, and $\tilde{n}(t)$ is the interference due to the channel noise.

Assuming that τ_1 has been estimated perfectly, the components of the observation vector $\mathbf{r} = (r_1, r_2, \ldots, r_{2N_s})$ are obtained through demodulation process as

$$r_{2k+1} = \int_0^{T_c} r\left(u + kT_f + c_k^{(1)}T_c + \tau_1\right) q(u)\, du \tag{37}$$

and

$$r_{2k+2} = \int_0^{T_c} r\left(u + kT_f + c_k^{(1)}T_c + \tau_1\right) q\left(u - \frac{T_c}{2}\right) du \tag{38}$$

for $k = 0, 1, \ldots, N_s - 1$, which can be obtained from Fig. 1 by letting $T_s = N_s T_f$, $N = 2N_s$, and $\psi_i(t) = q(t - Q_i T_f - c_k^{(1)} T_c - R_i T_c/2 - \tau_1)$ for $i = 1, 2, \ldots, N$. Here, Q_i and R_i are the quotient and remainder of i when divided by 2, respectively. Now, the detector is to choose between

$$H_1 : \begin{cases} r_{2k+1} = \theta + n_{2k+1} \\ r_{2k+2} = n_{2k+2} \end{cases} \tag{39}$$

and

$$H_2 : \begin{cases} r_{2k+1} = n_{2k+1} \\ r_{2k+2} = \theta + n_{2k+2} \end{cases} \tag{40}$$

for $k = 0, 1, \ldots, N_s - 1$. Here, H_i denotes the hypothesis that $s_i^{(1)}(t)$ is transmitted, $\theta = A_1\tilde{\theta}$, and

$$n_{2k+1} = \int_0^{T_c} n\left(u + kT_f + c_k^{(1)}T_c + \tau_1\right) q(u)\, du \tag{41}$$

and

$$n_{2k+2} = \int_0^{T_c} n\left(u + kT_f + c_k^{(1)}T_c + \tau_1\right) q\left(u - \frac{T_c}{2}\right) du \tag{42}$$

are the interference components of the observation vector $\mathbf{r}$.

B. Detectors for Impulsive Interference

In this section, we obtain specific expressions for the detectors (decision regions) under some models of impulsive interference.

1) Detectors for Bivariate Isotropic SαS Interference: The SαS distribution, an elegant model for impulsive interference, has been tested with a variety of real data and found to match the data with high fidelity [8], [12], [14]. Let $\{(n_{2k+1}, n_{2k+2})\}_{k=0}^{N_s-1}$ be i.i.d. bivariate random vectors, of which the common pdf of $\underline{n} = (n_{2k+1}, n_{2k+2})$ is the bivariate isotropic SαS (BISαS) pdf

$$f_{\underline{n}}(x,y) = \begin{cases} \frac{1}{\pi^2\gamma^{2/\alpha}} \sum_{k=1}^{\infty} \frac{2^{\alpha k}(-1)^{k-1}}{k!} \\ \quad \cdot\Gamma^2\left(\frac{\alpha k}{2}+1\right)\sin\left(\frac{k\alpha\pi}{2}\right) \\ \quad \cdot\left(\frac{\sqrt{x^2+y^2}}{\gamma^{1/\alpha}}\right)^{-\alpha k-2}, & 0<\alpha\le 1 \\ \frac{1}{2\pi\alpha\gamma^{2/\alpha}}\sum_{k=0}^{\infty}\frac{1}{(k!)^2}\Gamma\left(\frac{2k+2}{\alpha}\right) \\ \quad \cdot\left(-\frac{x^2+y^2}{4\gamma^{2/\alpha}}\right)^k, & 1\le\alpha\le 2. \end{cases} \tag{43}$$

Clearly, n_{2k+1} and n_{2k+2} are correlated in general. In (43), the dispersion parameter $\gamma > 0$ is related to the spread of the BISαS pdf, and the characteristic exponent $\alpha, 0 < \alpha \le 2$ is related to the heaviness of the tails of the BISαS pdf with a smaller value indicating a heavier tail. It is shown in Appendix C that the two infinite series in (43) result in the bivariate Cauchy pdf

$$f_{\underline{n}}(x,y) = \frac{\gamma}{2\pi(x^2+y^2+\gamma^2)^{3/2}} \tag{44}$$

when $\alpha = 1$, and the second infinite series in (43) becomes the Gaussian pdf

$$f_{\underline{n}}(x,y) = \frac{1}{4\pi\gamma}\exp\left\{-\frac{x^2+y^2}{4\gamma}\right\} \tag{45}$$

when $\alpha = 2$. Under this Gaussian assumption, we get the decision region

$$D_1^{\mathrm{ML},G} = \left\{\mathbf{r} : \sum_{k=0}^{N_s-1}(r_{2k+1} - r_{2k+2}) \ge 0\right\} \tag{46}$$

of the GO detector with the ML criterion. Clearly, $D_2^{\mathrm{ML},G}$ is obtained by reversing the inequality in (46).

For the BISαS distributions, in general, the lack of closed-form expressions prohibits the computations of optimum detectors, except for the Gaussian and Cauchy distributions [11]. Thus, the optimum detector for the Cauchy distribution, the Cauchy-optimized (CO) detector, has been used often as a useful detector under the general impulsive pdf (43). After some manipulations, we get

$$D_1^{\mathrm{ML},C} = \left\{\mathbf{r} : \prod_{k=0}^{N_s-1}\frac{r_{2k+1}^2 + (r_{2k+2}-\theta)^2 + \gamma^2}{(r_{2k+1}-\theta)^2 + r_{2k+2}^2 + \gamma^2} \ge 1\right\} \tag{47}$$

for the CO detector. Again, $D_2^{\mathrm{ML},C}$ is obtained by reversing the inequality in (47). Clearly, the CO detector based on (47) should first estimate the values of γ and θ for optimum performance.

Similarly, the decision region of the proposed detector under the Cauchy environment is

$$D_1^{P,C} = \left\{\mathbf{r} : \sum_{k=0}^{N_s-1}\frac{r_{2k+1} - r_{2k+2}}{r_{2k+1}^2 + r_{2k+2}^2 + \gamma^2} \ge 0\right\} \tag{48}$$

for which the estimation of θ is unnecessary. Although the parameter γ has still to be estimated, it can be obtained easily, for example, by computing the sample mean and sample variance of independent realizations of a BISαS process [15].

2) Detectors for SαS Interference: We now consider the case where n_{2k+1} and n_{2k+2} are independent: It is now assumed that $\{n_{2k+1}\}_{k=1}^{N_s}$ and $\{n_{2k+2}\}_{k=1}^{N_s}$ are all i.i.d. SαS random variables with the pdf

$$f(x) = \begin{cases} \frac{1}{\pi\gamma^{1/\alpha}}\sum_{k=1}^{\infty}\frac{(-1)^{k-1}}{k!}\Gamma(\alpha k+1) \\ \quad \cdot\sin\left(\frac{k\alpha\pi}{2}\right)\left(\frac{|x|}{\gamma^{1/\alpha}}\right)^{-\alpha k-1}, & 0<\alpha\le 1 \\ \frac{1}{\pi\alpha\gamma^{1/\alpha}}\sum_{k=0}^{\infty}\frac{(-1)^k}{(2k)!} \\ \quad \cdot\Gamma\left(\frac{2k+1}{\alpha}\right)\left(\frac{x}{\gamma^{1/\alpha}}\right)^{2k}, & 1\le\alpha\le 2. \end{cases} \tag{49}$$

When $\alpha = 1$, the ML criterion results in the decision region

$$D_1^{\mathrm{ML},C} = \left\{ \mathbf{r} : \prod_{k=0}^{N_s-1} (r_{2k+1}^2 + \gamma^2)\{(r_{2k+2} - \theta)^2 + \gamma^2\} \geq \prod_{k=0}^{N_s-1} (r_{2k+2}^2 + \gamma^2)\{(r_{2k+1} - \theta)^2 + \gamma^2\} \right\} \quad (50)$$

and the proposed criterion produces

$$D_1^{P,C} = \left\{ \mathbf{r} : \sum_{k=0}^{N_s-1} \left(\frac{r_{2k+1}}{r_{2k+1}^2 + \gamma^2} - \frac{r_{2k+2}}{r_{2k+2}^2 + \gamma^2} \right) \geq 0 \right\}. \quad (51)$$

3) Detectors for Bivariate t-Distributed Interference: Assume the bivariate t-pdf [3], [12]

$$f_{\underline{n}}(x, y) = \frac{1}{2\pi\sigma^2\sqrt{1-\rho^2}} \left(1 + \frac{x^2 - 2\rho xy + y^2}{\sigma^2\eta(1-\rho^2)} \right)^{-\frac{\eta+2}{2}} \quad (52)$$

for $\underline{n} = (n_{2k+1}, n_{2k+2})$, where ρ is the correlation coefficient, η denotes the rate of decay of the pdf with a smaller value representing a more impulsive pdf, and σ^2 determines (together with η) the variance. As $\eta \to \infty$, (52) approaches the bivariate Gaussian pdf. After some manipulations, it is straightforward to obtain (53) and (54), shown at the bottom of the next page.

4) Detectors for Univariate t-Distributed Interference: Assume that $\{n_{2k+1}\}_{k=1}^{N_s}$ and $\{n_{2k+2}\}_{k=1}^{N_s}$ are i.i.d. t-distributed random variables with the common pdf (27). Then, the ML criterion results in (55), shown at the bottom of the next page, and the proposed criterion gives

$$D_1^{P,t} = \left\{ \mathbf{r} : \sum_{k=0}^{N_s-1} \left(\frac{r_{2k+1}}{\nu + r_{2k+1}^2} - \frac{r_{2k+2}}{\nu + r_{2k+2}^2} \right) \geq 0 \right\}. \quad (56)$$

C. Numerical Results

Since the variance of the SαS distribution with $\alpha < 2$ is not defined, the standard SNR becomes meaningless. Instead, the geometric SNR (G-SNR) can be used [16] to indicate the relative strength between the information-bearing signal and SαS process. The G-SNR is defined as

$$\text{G-SNR} = \frac{\theta^2}{2C_g^{-1+2/\alpha}\gamma^{2/\alpha}} \quad (57)$$

where $C_g = \exp\{\lim_{s\to\infty}(\sum_{z=1}^{s}(1)/(z) - \ln s)\} \simeq 1.78$. Note that for the Gaussian case ($\alpha = 2$), the definition of G-SNR is consistent with that of the standard SNR.

Figs. 4 and 5 show the performance characteristics of the proposed (47), CO (47), and GO (46) detectors in the BISαS interference environment with $\alpha = 1$ and $\alpha = 2$, respectively. The G-SNR is shown in its square root value not in dB to emphasize the low G-SNR regions in these figures (and in Figs. 6–9). It is observed that when the CO detector has estimated the value of θ inaccurately, its performance would be worse than that of the proposed detector even in the Cauchy environment. The performance of the proposed detector hardly differs from that of the CO detector, especially when the G-SNR is close to zero. Since the proposed criterion is guaranteed to minimize the error probability when the signal strength approaches zero, the performance of the proposed detector could become worse than that of the CO detector when the G-SNR is high; however, the performance gap between the CO and proposed detectors decreases as the number N_s of UWB pulses per symbol increases. Thus, the two detectors will result in almost the same performance for practical values (several hundreds) of N_s. Clearly, although the GO detector outperforms the other two detectors in the Gaussian environment (Fig. 5), it fails to work adequately in the Cauchy environment (Fig. 4).

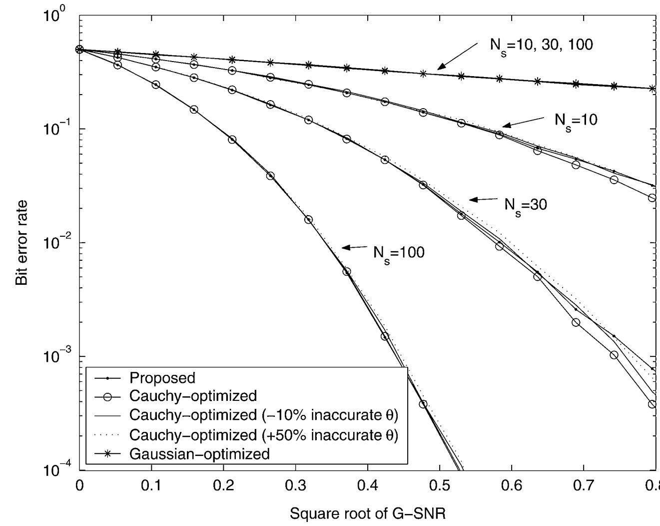

Fig. 4. Performance comparison of the proposed (48), CO (47), and GO (46) detectors in the Cauchy (BISαS with $\alpha = 1$) environment (44): The performance of the CO detector with θ estimated inaccurately is also included.

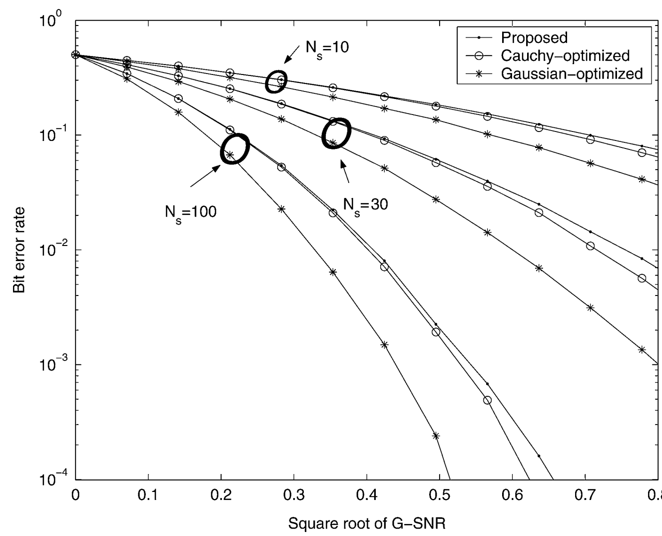

Fig. 5. Performance comparison of the proposed (48), CO (47), and GO (46) detectors in the Gaussian (BISαS with $\alpha = 2$) environment (45).

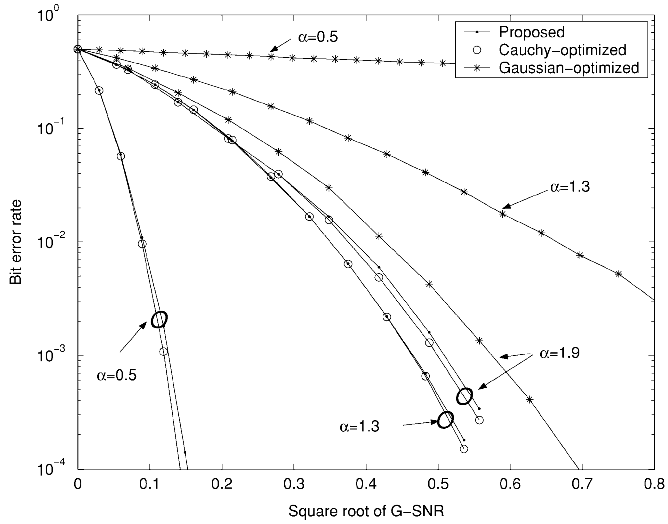

Fig. 6. Performance comparison of the proposed (48), CO (47), and GO (46) detectors when $N_s = 100$ in the BISαS environment (43) with $\alpha = 0.5, \alpha = 1.3$, and $\alpha = 1.9$.

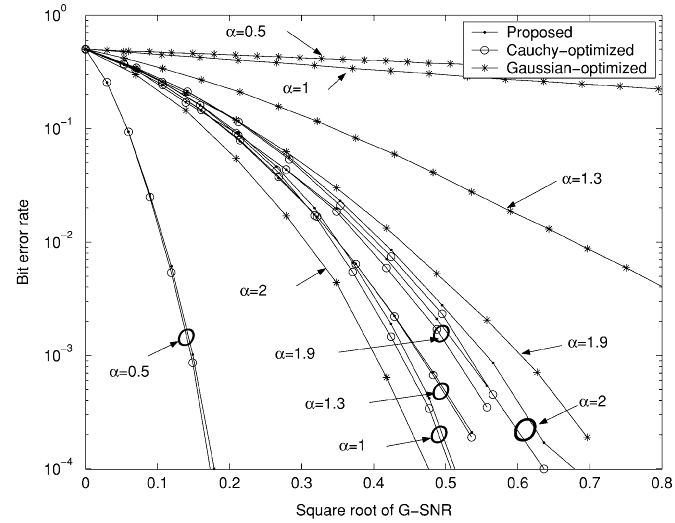

Fig. 7. Performance comparison of the proposed (51), CO (50), and GO (46) detectors with $N_s = 100$ in the SαS environment (49) when $\alpha = 0.5, \alpha = 1, \alpha = 1.3, \alpha = 1.9$, and $\alpha = 2$.

From the bit error rate curves of the three detectors for $N_s = 100$ and various values of α as shown in Figs. 4–6, it is clear that the proposed detector shows almost the same performance as the CO detector. In addition, the proposed detector outperforms the GO detector at all the values of the characteristic exponents considered here, except for the case $\alpha = 2$, at which value the GO detector is obviously the optimum. For smaller values of the characteristic exponent (that is, for more impulsive interference cases), the GO detector becomes almost useless, while the proposed and CO detectors maintain acceptable performance.

Fig. 7 shows the performance difference among the proposed (51), CO (50), and GO (46) detectors in the univariate SαS interference model (49) when $N_s = 100$. As in the BISαS environment, the proposed detector exhibits almost the same performance as the CO detector and outperforms the GO detector.

Fig. 8 shows how the three detectors specified by (46), (53), and (54) perform in the bivariate t-distributed impulsive interference (52) when $\rho = 0.3$ and $N_s = 100$. The proposed detector shows practically the same performance as the optimum detector and is superior to the GO detector. It is also observed that such a general characteristic of the three detectors does not change except $\eta \to \infty$. Similar observations can be made also in the case of the univariate t-distributed interference (27), as shown in Fig. 9.

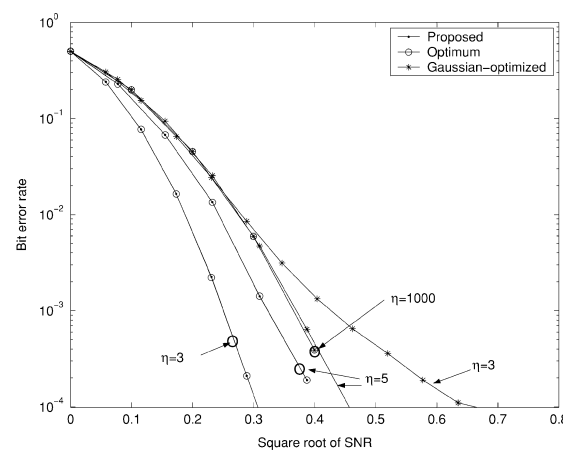

Fig. 8. Performance comparison of the proposed (54), optimum (53) and GO (46) detectors in the bivariate t-distributed impulsive model (52) when $N_s = 100$ and $\rho = 0.3$.

$$D_1^{\mathrm{ML},t} = \left\{ \mathbf{r} : \prod_{k=0}^{N_s-1} \frac{\sigma^2\eta(1-\rho^2) + r_{2k+1}^2 - 2\rho r_{2k+1}(r_{2k+2}-\theta) + (r_{2k+2}-\theta)^2}{\sigma^2\eta(1-\rho^2) + (r_{2k+1}-\theta)^2 - 2\rho r_{2k+2}(r_{2k+1}-\theta) + r_{2k+2}^2} \geq 1 \right\} \tag{53}$$

$$D_1^{P,t} = \left\{ \mathbf{r} : \sum_{k=0}^{N_s-1} \frac{r_{2k+1} - r_{2k+2}}{\sigma^2\eta(1-\rho^2) + r_{2k+1}^2 - 2\rho r_{2k+1} r_{2k+2} + r_{2k+2}^2} \geq 0 \right\} \tag{54}$$

$$D_1^{\mathrm{ML},t} = \left\{ \mathbf{r} : \prod_{k=0}^{N_s-1} \frac{(1 + r_{2k+1}^2/\nu)\{1 + (r_{2k+2}-\theta)^2/\nu\}}{(1 + r_{2k+2}^2/\nu)\{1 + (r_{2k+1}-\theta)^2/\nu\}} \geq 1 \right\} \tag{55}$$

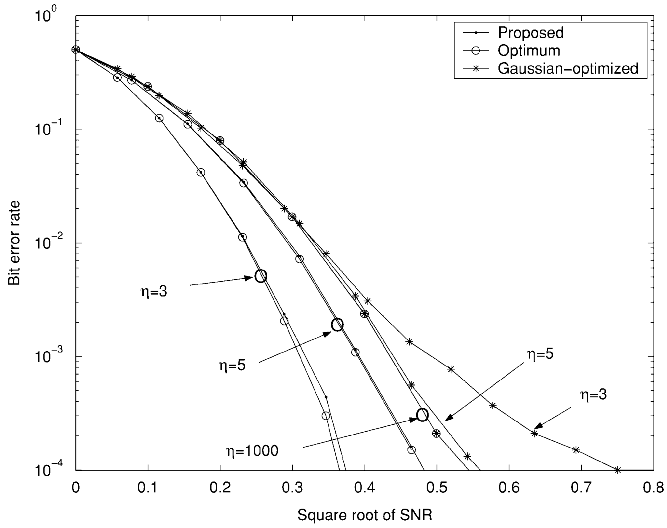

Fig. 9. Performance comparison of the proposed (56), optimum (55), and GO (46) detectors in the univariate t-distributed impulsive model (27) when $N_s = 100$ and $\rho = 0.3$.

In short, it is anticipated that a specific choice of the impulsive interference model does not, in general, have an influence on the relative performance of the proposed, optimum, and GO detectors. Note that the proposed detector offers almost the same performance as the optimum detector with reduced complexity and exhibits higher performance than the GO detector in impulsive interference.

IV. Conclusion

The criterion proposed in this paper for weak m-ary signal detection is designed to be optimum in the sense of minimizing the error probability when the signals are of weak strengths. It is shown that the proposed criterion has exactly the same performance as the ML criterion if, for example, the joint pdf of noise components is a monotonically decreasing function of the sum of the noise components squared and the signals are of equienergy. The proposed criterion relieves us from the requirement of estimating the signal strength and, consequently, results in simpler detector structures.

Based on the proposed criterion, a detector has been proposed for the UWB-MA system in the presence of impulsive interference. Numerical results demonstrate that the proposed detector possesses less complexity than and almost the same performance as the optimal detector and outperforms the GO detector in impulsive interference.

We have assumed that signals experience linear distortion in this paper. Further study based on the proposed criterion is therefore anticipated in more general environment with nonlinear distortion and/or time-varying frequency-selective fading. For instance, employing a more realistic UWB channel model [17], [18], rake receivers are analyzed under impulsive multipath circumstances in [19]: The proposed criterion is again observed to result in effective detectors in the UWB channel employed.

Appendix A

Examples of Signaling Schemes

1) On-off keyed (OOK) signals ($N = 1$): When $u(t)$ is a unit energy signal with duration T_s [for example, $u(t) = \cos(2\pi f t)/\sqrt{T_s}$ with $f \gg T_s$], let $s_1(t) = \theta u(t)$ and $s_2(t) = 0$. We then have $\psi_1(t) = u(t)$, $\epsilon_1 = 1$, $\epsilon_2 = 0$, $s_{11} = 1$, and $s_{21} = 1$.
2) PSK signals ($N = 2$): For $i = 1, 2, \ldots, M$, let $s_i(t) = (\theta)/(\sqrt{T_s}) \cos(2\pi f t + 2\pi i/M)$, $f \gg T_s$. With $\psi_1(t) = \cos(2\pi f t)/\sqrt{T_s}$ and $\psi_2(t) = -\sin(2\pi f t)/\sqrt{T_s}$, we have $s_{i1} = \cos(2\pi i/M)$, $s_{i2} = \sin(2\pi i/M)$, and $\epsilon_i = 1$ for $i = 1, 2, \ldots, M$.
3) QAM signals ($N = 2$): For $i = 1, 2, \ldots, M$, let $s_i(t) = (\theta A_{i1})/(\sqrt{T_s}) \cos(2\pi f t) + (\theta A_{i2})/(\sqrt{T_s}) \sin(2\pi f t)$, $f \gg T_s$. Here, $\{(A_{i1}, A_{i2})\}_{i=1}^{M}$ represents M points in the two dimensional real space. With the basis functions $\psi_1(t) = \cos(2\pi f t)/\sqrt{T_s}$ and $\psi_2(t) = \sin(2\pi f t)/\sqrt{T_s}$, we have $s_{i1} = A_{i1}/\sqrt{A_{i1}^2 + A_{i2}^2}$, $s_{i2} = A_{i2}/\sqrt{A_{i1}^2 + A_{i2}^2}$, and $\epsilon_i = \sqrt{A_{i1}^2 + A_{i2}^2}$ for $i = 1, 2, \ldots, M$.
4) Orthogonal signals [$N = M$; the frequency shift keyed (FSK) and PPM signals belong to this class]: When $\tilde{u}(t)$ is a unit energy signal with duration T_s/M, let

$$s_i(t) = \frac{\theta}{\sqrt{T_s}} \cos\{2\pi(f + m\Delta f)t\} \tag{58}$$

with $\Delta f = 1/(2T_s)$ and $f \gg T_s$ for the FSK signals, and

$$s_i(t) = \theta \tilde{u}\{t - (m-1)T_s/M\} \tag{59}$$

for the PPM signals, where $i = 1, 2, \ldots, M$. With the basis functions $\psi_k(t) = \cos\{2\pi(f + k\Delta f)t\}/\sqrt{T_s}, k = 1, 2, \ldots, N$ for FSK signals and $\psi_k(t) = \tilde{u}\{t - (k-1)T_s/N\}, k = 1, 2, \ldots, N$ for PPM signals, we have $\epsilon_i = 1, i = 1, 2, \ldots, M$ and $s_{ik} = 1$ for $k = i$ and $s_{ik} = 0$ for $k \neq i$.

Appendix B

Decision Regions for Specific Signaling Schemes and Interference Models

The LO nonlinearity $g_{\text{LO}}(\cdot)$ [2], [3] for the Gaussian, univariate Cauchy, and logistic noise are $g_G(x) = (x)(\sigma^2)$, $g_C(x) = (2x)/(x^2 + \gamma^2)$, and $g_L(x) = (b(1 - e^{-bx}))/(1 + e^{-bx})$, respectively. Then, from the results in Section II-C and the quantities shown in Appendix A, we have the following results.

OOK Signals: In the Gaussian, univariate Cauchy, and logistic noise, we have $D_1^{\text{ML}} = \{\mathbf{r} : r_1 \geq \theta/2\}$, $D_2^{\text{ML}} = \{\mathbf{r} : r_1 \leq \theta/2\}$, $D_1^P = \{\mathbf{r} : r_1 \geq 0\}$, and $D_2^P = \{\mathbf{r} : r_1 \leq 0\}$.

PSK Signals: We have

$$D_i^P = \left\{ \mathbf{r} : g_{\text{LO}}(r_1) \cos \frac{2\pi i}{M} + g_{\text{LO}}(r_2) \sin \frac{2\pi i}{M} \right.$$
$$\left. \geq g_{\text{LO}}(r_1) \cos \frac{2\pi j}{M} + g_{\text{LO}}(r_2) \sin \frac{2\pi j}{M}, \quad \forall j \right\}$$

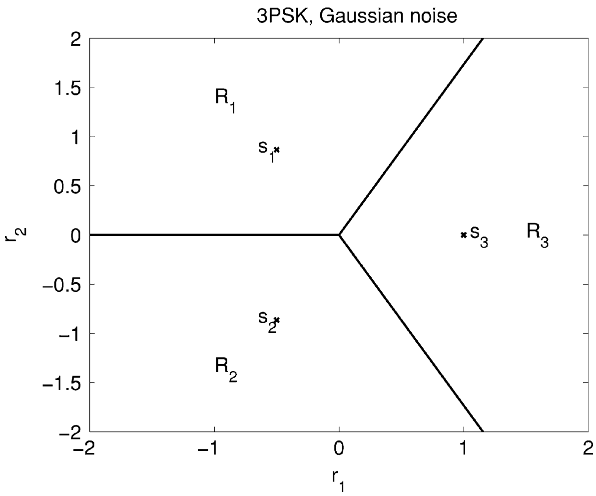

Fig. 10. Decision regions for 3PSK signaling in Gaussian noise.

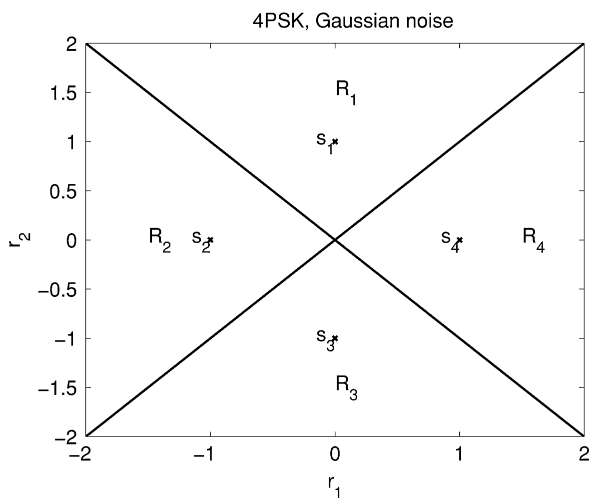

Fig. 11. Decision regions for 4PSK signaling in Gaussian noise.

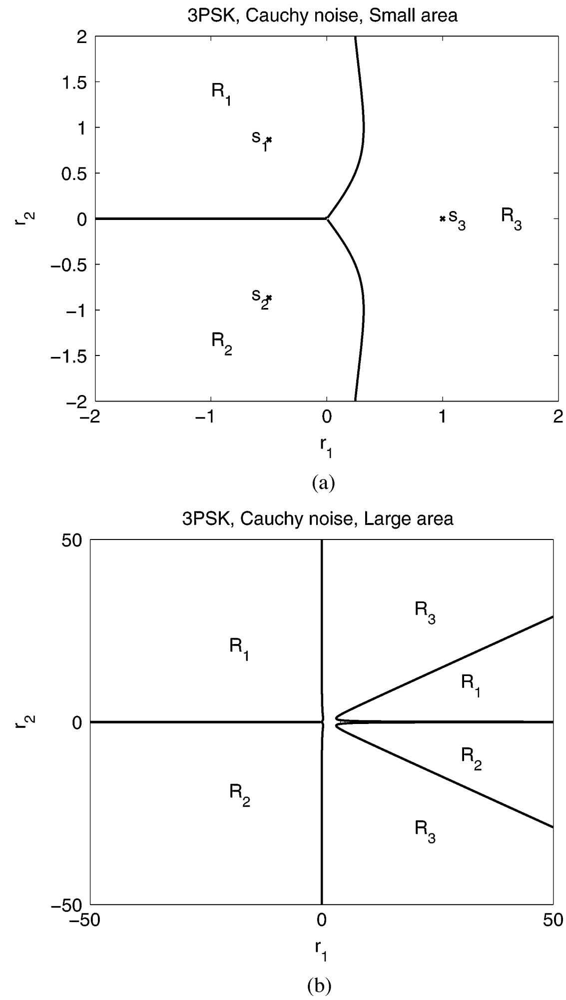

Fig. 12. Decision regions for 3PSK signaling in the univariate Cauchy noise when $\gamma = 1$ [the boundary curves are defined by $\sqrt{3}r_1(r_1^2 + r_2^2) \pm r_2(r_1^2 + \gamma^2) = 0$ when $r_1 > 0$, which becomes $\sqrt{3}r_1 \pm r_2 = 0$ near the point $(r_1, r_2) = (0, 0)$). (a) 3PSK, Cauchy noise, small area. (b) 3PSK, Cauchy noise, large area.

$$= \left\{ \mathbf{r} : \left\{ \cos\frac{2\pi i}{M} - \cos\frac{2\pi j}{M} \right\} g_{\mathrm{LO}}(r_1) \geq -\left\{ \sin\frac{2\pi i}{M} - \sin\frac{2\pi j}{M} \right\} g_{\mathrm{LO}}(r_2) \right\}. \qquad (60)$$

Specifically, we have the following results.

a) In the Gaussian noise, we have (61), shown at the bottom of the next page. Clearly, for BPSK signals (i.e., when $M = 2$), $D_1^{\mathrm{ML}} = D_1^P = \{\mathbf{r} : r_1 \leq 0\}$ and $D_2^{\mathrm{ML}} = D_2^P = \{\mathbf{r} : r_1 \geq 0\}$. Decision regions for $M = 3$ and 4 are shown in Figs. 10 and 11, respectively, where R_i is used to denote D_i^P.

b) In the univariate Cauchy noise, we have (62) and (63), shown at the bottom of the next page. It is easy to see that the decision regions for BPSK signals are the same as those obtained for the Gaussian noise. When $M = 3$ and $M = 4$, the decision regions are as shown in Figs. 12 and 13, respectively. It should be noticed in these figures that the decision regions near the point $(r_1, r_2) = (0, 0)$ are almost the same as those for the Gaussian noise.

c) In the logistic noise, we have (64) and (65), shown at the bottom of the next page. It is straightforward to show that the decision regions when $M = 2$ and $M = 4$ in the logistic noise are almost the same as those when $M = 2$ and $M = 4$ in the Gaussian noise, respectively. Fig. 14 shows the decision regions when $M = 3$. Again, note that the decision regions near the point $(r_1, r_2) = (0, 0)$ are almost the same as those in the Gaussian noise.

QAM Signals: We have $D_i^P = \{\mathbf{r} : \sum_{k=1}^{2}(A_{ik} - A_{jk})g_{\mathrm{LO}}(r_k) \geq 0, \forall j\}$. Specifically, we have the following results.

a) In the Gaussian noise, $D_i^{\mathrm{ML}} = \{\mathbf{r} : \sum_{k=1}^{2}(A_{ik} - A_{jk})r_k \geq \sum_{k=1}^{2}((A_{ik}^2 - A_{jk}^2)\theta)/(2), \forall j\}$ and $D_i^P = \{\mathbf{r} : \sum_{k=1}^{2}(A_{ik} - A_{jk})r_k \geq 0, \forall j\}$. Note that we have $D_i^{\mathrm{ML}} = D_i^P$ when $A_{11}^2 + A_{12}^2 = A_{21}^2 + A_{22}^2$.

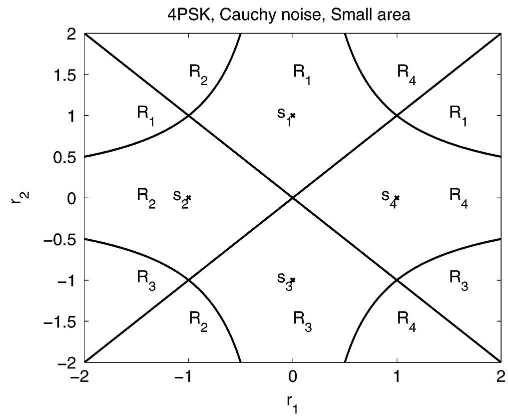

(a)

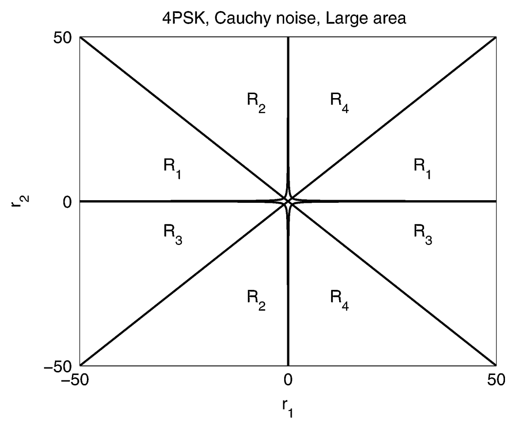

(b)

Fig. 13. Decision regions for 4PSK signaling in the univariate Cauchy noise when $\gamma = 1$ [the boundary curves are $r_2 = \pm r_1$ and $r_1 r_2 = \pm\gamma^2$]. (a) 3PSK, Cauchy noise, small area, (b) 3PSK, Cauchy noise, large area.

b) In the univariate Cauchy noise, $D_i^{\rm ML} = \{\mathbf{r} : \prod_{k=1}^2((r_k - \theta A_{ik})^2 + \gamma^2)/((r_k - \theta A_{jk})^2 + \gamma^2) \leq 1, \forall j\}$ and $D_i^P = \{\mathbf{r} : \sum_{k=1}^2((A_{ik} - A_{jk})r_k)/(r_k^2 + \gamma^2) \geq 0, \forall j\}$.

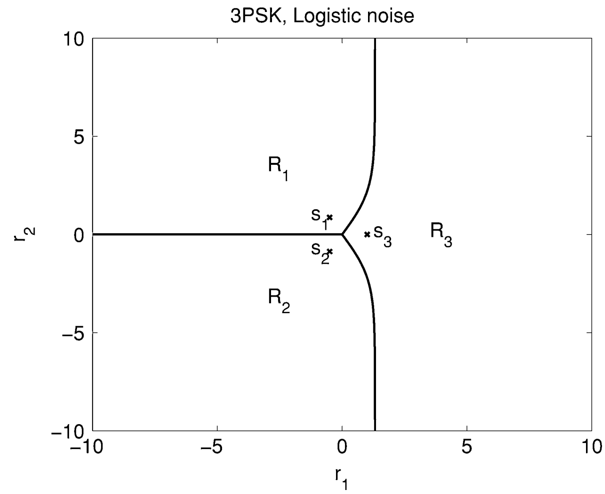

Fig. 14. Decision regions for 3PSK signaling in the logistic noise when $b = 1$. [The boundary curves are defined by $r_2 = \pm\ln((\sqrt{3}-1) - (\sqrt{3}+1)e^{r_1})/((\sqrt{3}-1)e^{r_1} - (\sqrt{3}+1))$ when $0 \leq r_1 \leq \ln(\sqrt{3}+1)/(\sqrt{3}-1)$, which becomes $r_2 \approx \pm((\sqrt{3}-1) - (\sqrt{3}+1)(1+r_1))/((\sqrt{3}-1)(1+r_1) - (\sqrt{3}+1)) - 1 = \pm(2\sqrt{3}r_1)/(-2+(\sqrt{3}-1)r_1) \approx \pm\sqrt{3}r_1$ near the point $(r_1, r_2) = (0, 0)$.]

c) In the logistic noise, $D_i^{\rm ML} = \{\mathbf{r} : \prod_{k=1}^2 e^{b\theta(A_{ik} - A_{jk})}((1 + e^{-b(r_k - \theta A_{jk})})^2)/((1 + e^{-b(r_k - \theta A_{ik})})^2) \geq 1, \forall j\}$ and $D_i^P = \{\mathbf{r} : \sum_{k=1}^2 (A_{ik} - A_{jk})(1 - e^{-br_k})/(1 + e^{-br_k}) \geq 0, \forall j\}$.

Orthogonal Signals: For orthogonal signals, we generally have $D_i^P = \{\mathbf{r} : g_{\rm LO}(r_i) \geq g_{\rm LO}(r_j), \forall j\}$. Specifically, we have the following results.

a) In the Gaussian and logistic noise, $D_i^{\rm ML} = D_i^P = \{\mathbf{r} : r_i \geq r_j, \forall j\}$.

b) In the univariate Cauchy noise, $D_i^{\rm ML} = \{\mathbf{r} : (r_i - \theta/2)/(r_i^2 + \gamma^2) \geq (r_j - \theta/2)/(r_j^2 + \gamma^2), \forall j\}$ and $D_i^P = \{\mathbf{r} : (r_i)/(r_i^2 + \gamma^2) \geq (r_j)/(r_j^2 + \gamma^2), \forall j\}$. An example of the decision regions when $M = 2$ and $\gamma = 1$ is shown in Fig. 15 Again, note that the decision regions near the

$$D_i^{\rm ML} = D_i^P = \left\{\mathbf{r} : \left\{r_2 \cos\frac{(i+j)\pi}{M} - r_1 \sin\frac{(i+j)\pi}{M}\right\} \sin\frac{(i-j)\pi}{M} \geq 0, \quad \forall j\right\} \tag{61}$$

$$D_i^{\rm ML} = \left\{\mathbf{r} : \frac{((r_1 - \theta\cos(2\pi i/M))^2 + \gamma^2)((r_2 - \theta\sin(2\pi i/M))^2 + \gamma^2)}{((r_1 - \theta\cos(2\pi j/M))^2 + \gamma^2)((r_2 - \theta\sin(2\pi j/M))^2 + \gamma^2)} \leq 1, \quad \forall j\right\} \tag{62}$$

$$D_i^P = \left\{\mathbf{r} : \left\{\frac{r_2}{r_2^2 + \gamma^2} \cos\frac{(i+j)\pi}{M} - \frac{r_1}{r_1^2 + \gamma^2} \sin\frac{(i+j)\pi}{M}\right\} \sin\frac{(i-j)\pi}{M} \geq 0, \quad \forall j\right\} \tag{63}$$

$$\begin{aligned} D_i^{\rm ML} = \Bigg\{\mathbf{r} : & \frac{e^{b\theta\cos(2\pi i/M)}}{\left(1 + e^{-b(r_1 - \theta\cos(2\pi i/M))}\right)^2} \frac{e^{b\theta\sin(2\pi i/M)}}{\left(1 + e^{-b(r_2 - \theta\sin(2\pi i/M))}\right)^2} \\ & \geq \frac{e^{b\theta\cos(2\pi j/M)}}{\left(1 + e^{-b(r_1 - \theta\cos(2\pi j/M))}\right)^2} \frac{e^{b\theta\sin(2\pi j/M)}}{\left(1 + e^{-b(r_2 - \theta\sin(2\pi j/M))}\right)^2}, \quad \forall j\Bigg\} \end{aligned} \tag{64}$$

$$D_i^P = \left\{\mathbf{r} : \left\{\frac{1 - e^{br_2}}{1 + e^{br_2}} \cos\frac{(i+j)\pi}{M} - \frac{1 - e^{br_1}}{1 + e^{br_1}} \sin\frac{(i+j)\pi}{M}\right\} \sin\frac{(i-j)\pi}{M} \geq 0, \quad \forall j\right\} \tag{65}$$

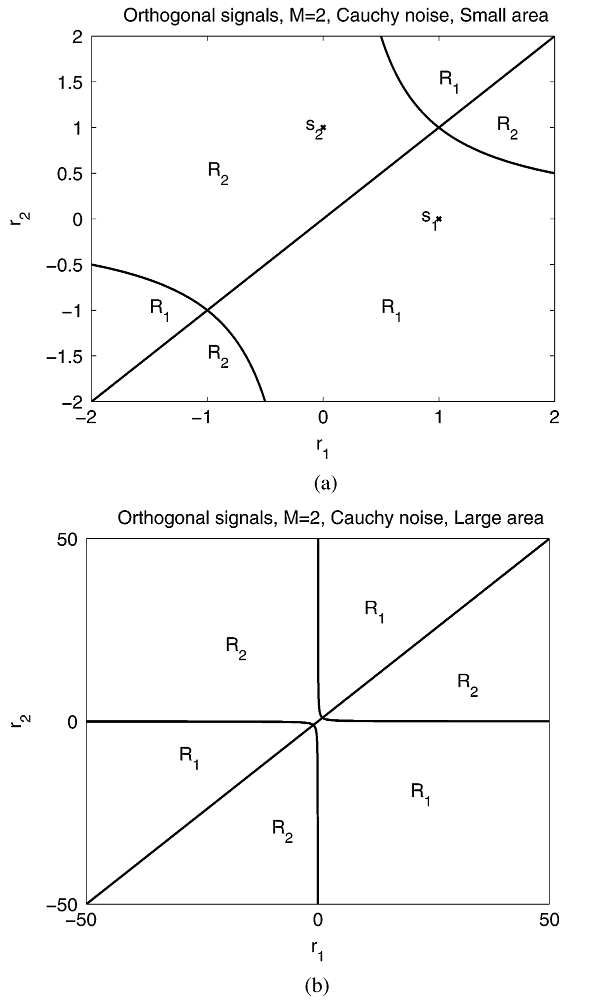

Fig. 15. Decision regions for orthogonal signaling in the univariate Cauchy noise when $M = 2$ and $\gamma = 1$.

point $(r_1, r_2) = (0, 0)$ are almost the same as those in the Gaussian noise.

APPENDIX C

When $\alpha = 1$, the first infinite series in (43) can be evaluated as

$$\begin{aligned} &\frac{1}{\pi^2\gamma^2}\sum_{k=1}^{\infty}\frac{2^k(-1)^{k-1}}{k!}\Gamma^2(k/2+1) \\ &\cdot \sin\left(\frac{k\pi}{2}\right)\left(\frac{\sqrt{x^2+y^2}}{\gamma}\right)^{-k-2} \\ &= \frac{1}{2\pi(x^2+y^2)}\cdot\frac{\gamma}{\sqrt{x^2+y^2}} \\ &\cdot\sum_{k=0}^{\infty}\frac{(-1)^k(2k+1)!}{2^{2k}(k!)^2}\left(\frac{\gamma^2}{x^2+y^2}\right)^k \\ &= \frac{\gamma}{2\pi(x^2+y^2+\gamma^2)^{3/2}} \end{aligned} \tag{66}$$

where we have used $\Gamma((2k+3)/(2)) = ((2k+1)!)/(2^{2k+1}k!)\sqrt{\pi}$ and

$$(1+x)^{-3/2} = \sum_{k=0}^{\infty}\frac{(-1)^k(2k+1)!}{2^{2k}(k!)^2}x^k. \tag{67}$$

The closed form expression (44) can also be obtained from the second infinite series in (43) when $\alpha = 1$. Specifically, again using (67), we have

$$\begin{aligned} &\frac{1}{2\pi\gamma^2}\sum_{k=0}^{\infty}\frac{\Gamma(2k+2)}{(k!)^2}\left(-\frac{x^2+y^2}{4\gamma^2}\right)^k \\ &= \frac{\gamma}{2\pi(x^2+y^2+\gamma^2)^{3/2}}. \end{aligned} \tag{68}$$

When $\alpha = 2$, the second infinite series in (43) becomes

$$\begin{aligned} &\frac{1}{4\pi\gamma}\sum_{k=0}^{\infty}\frac{\Gamma(k+1)}{(k!)^2}\left(-\frac{x^2+y^2}{4\gamma}\right)^k \\ &= \frac{1}{4\pi\gamma}\sum_{k=0}^{\infty}\frac{1}{k!}\left(-\frac{x^2+y^2}{4\gamma}\right)^k \end{aligned} \tag{69}$$

which is clearly the same as (45) since $\sum_{k=0}^{\infty}((-x)^k)/(k!) = e^{-x}$.

ACKNOWLEDGMENT

The authors would like to thank the anonymous reviewers for their helpful and constructive comments and suggestions.

REFERENCES

[1] J. Capon, “On the asymptotic efficiency of locally optimum detectors,” *IRE Trans. Inf. Theory*, vol. IT-7, no. 2, pp. 67–71, Apr. 1961.
[2] S. A. Kassam, *Signal Detection in Non-Gaussian Noise*. New York: Springer-Verlag, 1987.
[3] I. Song, J. Bae, and S. Y. Kim, *Advanced Theory of Signal Detection*. New York: Springer-Verlag, 2002.
[4] I. Song and S. A. Kassam, “Locally optimum rank detection of correlated random signals in additive noise,” *IEEE Trans. Inf. Theory*, vol. 38, no. 4, pp. 1311–1322, Jul. 1992.
[5] R. S. Blum and M. C. Deans, “Distributed random signal detection with multibit sensor decisions,” *IEEE Trans. Inf. Theory*, vol. 44, no. 2, pp. 516–524, Mar. 1998.
[6] E. Kokkinos and A. M. Maras, “Locally optimum Bayes detection in nonadditive first-order Markov noise,” *IEEE Trans. Commun.*, vol. 47, no. 3, pp. 387–396, Mar. 1999.
[7] J. Bae and I. Song, “Locally optimum rank detector test statistics for composite signals in generalized observations: One-sample case,” *IEICE Trans. Commun.*, vol. E85B, no. 11, pp. 2509–2511, Nov. 2002.
[8] C. L. Nikias and M. Shao, *Signal Processing with Alpha-Stable Distributions and Applications*. New York: Wiley, 1995.
[9] M. Z. Win and R. A. Scholtz, “Impulse radio: How it works,” *IEEE Commun. Lett.*, vol. 2, no. 2, pp. 36–38, Feb. 1998.
[10] ——, “Ultra-wide bandwidth time-hopping spread spectrum impulse radio for wireless multiple-access communications,” *IEEE Trans. Commun.*, vol. 48, no. 4, pp. 679–691, Apr. 2000.
[11] G. A. Tsihrintzis and C. L. Nikias, “Incoherent receiver in alpha-stable impulsive noise,” *IEEE Trans. Signal Process.*, vol. 43, no. 9, pp. 2225–2229, Sep. 1995.
[12] N. L. Johnson and S. Kotz, *Distributions in Statistics: Continuous Multivariate Distributions*. New York: Wiley, 1972.
[13] G. Samorodnitsky and M. S. Taqqu, *Non-Gaussian Random Processes: Stochastic Models with Infinite Variance*. London, U.K.: Chapman and Hall, 1994.
[14] Y. C. Yoon and R. Kohno, “Optimum multi-user detection in ultra-wideband (UWB) multiple-access communication systems,” in *Proc.*

IEEE Int. Communications Conf., vol. 2, New York, May 2002, pp. 812–816.

[15] R. Kapoor, A. Banerjee, G. A. Tsihrintzis, and N. Nandhakumar, “UWB radar detection of targets in foliage using alpha-stable clutter models,” *IEEE Trans. Aerosp. Electron. Syst.*, vol. 35, no. 3, pp. 819–834, Jul. 1999.

[16] T. C. Chuah, B. S. Sharif, and O. R. Hinton, “Nonlinear decorrelator for multiuser detection in non-Gaussian impulsive environments,” *Electron. Lett.*, vol. 36, no. 10, pp. 920–922, May 2000.

[17] A. Saleh and R. Valenzuela, “A statistical model for indoor multipath propagation,” *IEEE J. Sel. Areas Commun.*, vol. JSAC-5, no. 2, pp. 128–137, Feb. 1987.

[18] A. F. Molisch, J. R. Foerster, and M. Pendergrass, “Channel models for ultrawideband personal area networks,” *IEEE Trans. Wireless Commun.*, vol. 10, pp. 14–21, Dec. 2003.

[19] B. S. Kim, J. Bae, I. Song, S. Y. Kim, H. Kwon, and S. W. Choi, “A comparative analysis of optimum and suboptimum rake receivers in impulsive environment ultra wideband multiple access,” *IEEE Trans. Veh. Technol.*, submitted for publication.

Iickho Song (S’80–M’87–SM’96) was born in Seoul, Korea, in 1960. He received the B.S.E. (*magna cum laude*) and M.S.E. degrees in electronics engineering from Seoul National University in 1982 and 1984, respectively, and the M.S.E. and Ph.D. degrees in electrical engineering from the University of Pennsylvania, Philadelphia, in 1985 and 1987, respectively.

He was a Member of the Technical Staff at Bell Communications Research, Morristown, NJ, USA, in 1987. In 1988, he joined the Department of Electrical Engineering, Korea Advanced Institute of Science and Technology (KAIST), Daejon, Korea, where he is currently a Professor. He has coauthored *Advanced Theory of Signal Detection* (New York: Springer-Verlag, 2002) and *Random Processes* (Seoul: Saengneung, 2004) and has published a number of papers on signal detection and CDMA systems. His research interests include detection and estimation theory, statistical communication theory and signal processing, and mobile communications.

Prof. Song served as the Treasurer of the IEEE Korea Section in 1989. He has received many awards, including the Young Scientists Award presented by the President of the Republic of Korea in 2000.

Jinkyu Koo was born in Suweon, Korea, in 1980. He received the B.S.E. degree in electrical engineering from Korea University, Seoul, Korea, in 2001 and the M.S.E. degree in electrical engineering from Korea Advanced Institute of Science and Technology (KAIST), Daejeon, Korea, in 2004.

His research interests include next generation mobile radio communication system with special emphasis on physical layer design. His recent research is focused on ranging schemes for OFDMA-based systems.

Hyoungmoon Kwon (S’00) was born in Seoul, Korea, in 1976. He received the B.S. degree in electronics engineering from Yonsei University, Seoul, in 2000 and the M.S.E. degrees in electrical engineering from Korea Advanced Institute of Science and Technology (KAIST), Daejeon, Korea, in 2002, where he is currently working toward the Ph.D. degree.

He has been a Teaching and Research Assistant at the Department of Electrical Engineering, KAIST, since March 2000. His research interests include spread-spectrum systems and detection theory.

So Ryoung Park (S’99–M’03) was born in Daegu, Korea, in 1974. She received the B.S. degree in electronics engineering from Yonsei University, Seoul, Korea, in 1997 and the M.S.E. and Ph.D. degrees in electrical engineering from the Korea Institute of Science and Technology (KAIST), Daejeon, Korea, in 1999 and 2002, respectively.

She was a Research Assistant at the Department of Electrical Engineering, KAIST, from 1997 to 2001, and a Research Scientist at the Statistical Signal Processing Laboratory, Department of Electrical Engineering and Computer Science, KAIST, in 2002. She is currently an Assistant Professor at the School of Information, Communications, and Electronics Engineering, the Catholic University of Korea (CUK), Songsion, Korea. Her current research interests are in mobile communications and statistical signal processing with emphasis on spread spectrum communications

Prof. Park was the recipient of a Silver Prize and a Gold Prize at the Samsung Humantech Paper Contest in 1999 and 2001, respectively.

Sung Ro Lee was born in Koksung, Korea, in 1959. He received the B.S. degree in electronics engineering from Korea University, Seoul, Korea, in 1987 and the M.S.E. and Ph.D. degrees in electrical engineering from the Korea Institute of Science and Technology (KAIST), Daejeon, Korea, in 1990 and 1996, respectively.

He joined the Division of Information Engineering, Mokpo University, Mokpo, Korea, in 1997, where he is currently an Associate Professor. His research interests are in digital communication systems, wireless multimedia, and array signal processing.

Bo-Hyun Chung was born in Cheongju, Korea, in 1948. He received the B.S. and M.S. degrees in mathematics from Korea University, Seoul, Korea, in 1974 and 1984, respectively, and the Ph.D degree in mathematics from Hongik University, Seoul, in 1991.

He joined the Mathematics Section, College of Science and Technology, Hongik University, in 1991, where he has been teaching applied mathematics for science and engineering and is currently an Associate Professor. He has coauthored *Engineering Mathematics* (Seoul: Hyoungseol, 1997) and *Applied Mathematics for Science and Engineering* (Seoul: Keulnamu, 2005), and published a number of papers in Korean and international journals. His work has aroused interest in applications of extremal length. His research interests center on complex analysis and geometric function theory.